SUPPLEMENTARY MATERIAL

Comparison of single and dual energy CT for stopping power determination in proton therapy of head and neck cancer

S1 DECT-based SPR: Parametrization method

The DECT-based SPR method used in this study was proposed by Taasti *et al.* [1]. We have though made a few modifications to this method to further improve its robustness. The tissue classification was changed to reduce the risk of mis-classification and the optimization method for finding the fitting parameters for the SPR estimation equations was modified.

S1.1 Tissue classification

In this study, the tissue classification was performed using a nearest neighbor classifier [2] with three nearest neighbors. The calibration of this method was performed using the *fitcknn* function in MATLAB (The MathWorks Inc., Natick, MA), and based on the estimated CT numbers and a theoretical tissue classification for 71 reference human tissues listed by Schneider *et al.* [3]. This list was extended with replica of these tissues with image noise added to their estimated CT numbers.

The noise was sampled from a normal distribution with a mean of zero and a standard deviation equal to the noise level in the CT images of the patients. The noise level was determined by placing a few ROIs in homogeneous soft tissue regions of the patient images. The noise level was nearly the same for all patients and the same standard deviation was therefore used for all fourteen patients, $\sigma = [20, 20]$ HU. It is not assumed that the applied noise level is of great importance. 10,000 noise realizations were added to each tissue.

The theoretical tissue classification into soft and bone tissues was based on the elemental weight fraction of calcium. Tissues with a weight fraction of calcium higher than 1.5% was classified as bone tissues. The tissues with added image noise inherited the tissue classification from their noise-free counterpart, as image noise does not change the composition of a tissue only its CT number.

S1.2 SPR calibration

The optimization for finding the fitting parameters, $\boldsymbol{x}$, in the SPR estimation, Eq. (1) in the main text, was modified slightly. It was originally suggested to bound the fitting parameters to the interval $x_i \in [-15, 15]$ to ensure the parameters did not grow to large as this decreased the noise robustness of the SPR estimation [1]. In this study, a regularized fit was used instead of a bound on the fitting parameter values. The fitting parameters, $\boldsymbol{x}$, for each tissue group, tg (that is the soft or bone tissue group), was then fitted using the *lsqnonlin* function in MATLAB on the following equation:

$$\min_{\boldsymbol{x}} \left(\sum_{j=1}^{N} \left(\frac{\mathrm{SPR}^{tg}_{\mathrm{est},j}(\boldsymbol{x}) - \mathrm{SPR}_{\mathrm{theo},j}}{\mathrm{SPR}_{\mathrm{theo},j}} \cdot 100\% \right)^2 + \lambda \cdot \sum_{i=1}^{4} x_i^2 \right) \tag{S1}$$

The first term in this equation is a relative residual term, where the estimated SPR, $\mathrm{SPR}^{tg}_{\mathrm{est},j}$, is calculated using Eq. (1a) or (1b), and the theoretical SPR, $\mathrm{SPR}_{\mathrm{theo}}$, is calculated using the Bethe equation (see Eq. (3) in Ref. [4]). N is the number of tissues in each tissue group. We performed the fit on the 71 reference tissues, giving 46 soft tissues and 25 bone tissues using the theoretical tissue classification described in previous section. The second term is a regularization term, in this study we used a regularization parameter $\lambda = 10^{-2}$.

SPR calculations were performed assuming an initial proton energy of 200 MeV, and the mean ionization energy of water calculated using the Bragg additivity rule [4], $I_{\mathrm{w}} = 75.3$ eV.

The fitting parameters, x_i, used in this study is given in Table S1.I.

Table S1.I: Fitting parameters, x_i, for the SPR estimation in Eq. (1) in the main text. Group A: Siemens Flash, Dual Source scanner. Group B: Philips Big Bore, SECT scanner.

	Group A		**Group B**	
	Soft	Bone	Soft	Bone
x_1	0.0100	-0.0133	0.0100	-0.0134
x_2	2.8639	1.4595	4.0348	2.1654
x_3	0.9307	0.0701	1.1835	0.0707
x_4	-0.9006	0.3788	-1.1533	0.5860

S1.3 Effective energies

To calculate the reduced CT numbers in Eq. (2) in the main text the fitting parameters A_j^{tg} and B_j^{tg} have to be obtained in an optimization procedure using a set of tissue substitutes with known density and elemental composition. It was suggested by Taasti *et al.* to find one effective energy which characterized the entire x-ray spectrum [1]. This procedure was also used in this study, however, two effective energies were found for each spectrum, one for soft tissues and one for bone tissues, and then the fitting parameters, A_j^{tg} and B_j^{tg}, for each tissue group were found along with the effective energies, $E_{\mathrm{eff},j}^{tg}$:

$$\frac{\mu(E_{\mathrm{eff},j}^{tg})}{\mu_{\mathrm{w}}(E_{\mathrm{eff},j}^{tg})} = \frac{\mathcal{H}_j - B_j^{tg}}{A_j^{tg}} \tag{S2}$$

Here μ and μ_{w} are the attenuation coefficients for the material and water, respectively. This optimization was based on the CT numbers, $\mathcal{H}_j$, for the tissue substitutes of the Gammex Cone-Beam Electron Density Phantom (Gammex Inc., Middleton, WI).

The effective energies and the corresponding fitting parameters are listed in Table S1.II.

Table S1.II: Effective energies, E_{eff}, and corresponding fitting parameters, A and B from Eq. (S2) for each x-ray energy spectrum (low and high energy) for the two patient groups. Group A: Siemens Flash, Dual Source scanner. Group B: Philips Big Bore, SECT scanner.

	Group A		**Group B**	
	100 kVp	Sn140 kVp	90 kVp	140 kVp
$E_{\mathrm{eff}}^{\mathrm{soft}}$ (keV)	63	94	65	85
$E_{\mathrm{eff}}^{\mathrm{bone}}$ (keV)	75	107	86	112
A^{soft}	998.5	999.2	973.5	970.9
B^{soft}	-996.3	-996.1	-970.1	-969.2
A^{bone}	1146.7	1109.2	1403.5	1291.1
B^{bone}	-1140.9	-1096.2	-1350.4	-1254.2

S2 SECT-based SPR: Stoichiometric method

We calibrated the SECT-based stoichiometric conversion curve for each CT scanner individually, but the two curves were defined in the same way, i.e. having the same number of kinks and connection lines, whereby only the slopes of the line segments could differ. The conversion curves were calibrated based on the 71 reference human tissues. The conversion curve for the Dual Source CT scanner is seen in Figure S2.A.

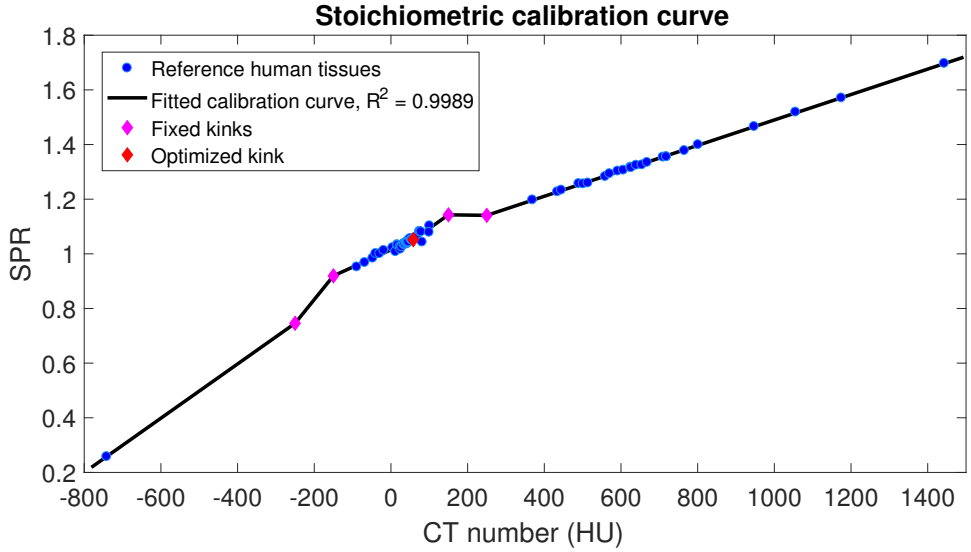

Figure S2.A: CT-to-SPR conversion curve used for SECT-based SPR estimation for patient Group A.

References

[1] V. T. Taasti, J. B. B. Petersen, L. P. Muren, J. Thygesen, and D. C. Hansen. A robust empirical parametrization of proton stopping power using dual energy CT. *Med. Phys.*, 43: 5547–5560, 2016.

[2] T. Cover and P. Hart. Nearest neighbor pattern classification. *IEEE Trans. Inf. Theory*, 13: 21–27, 1967.

[3] W. Schneider, T. Bortfeld, and W. Schlegel. Correlation between CT numbers and tissue parameters needed for Monte Carlo simulations of clinical dose distributions. *Phys. Med. Biol.*, 45: 459–478, 2000.

[4] U. Schneider, E. Pedroni, and A. Lomax. The calibration of CT Hounsfield units for radiotherapy treatment planning. *Phys. Med. Biol.*, 41: 111–124, 1996.